

## Article

# Three-Dimensional Printing Materials for Cultural Innovation Products of Historical Buildings

Hao Hu <sup>1</sup>, Xiaoxiao Cao <sup>1,2,\*</sup> , Tao Zhang <sup>3</sup>, Zhenfu Chen <sup>4</sup> and Jinliang Xie <sup>4</sup>
<sup>1</sup> Department of Product Design, Communication University of Zhejiang, 998 Xueyuan Street, Qiantang District, Hangzhou 310018, China; 20170001@cuz.edu.cn

<sup>2</sup> System Planning Lab, Chiba University, 1-33 Yayoicho, Chiba-shi 263-8522, Chiba, Japan

<sup>3</sup> Department of Product Design, Zhejiang Sci-Tech University, 928 No. 2 Street, Qiantang District, Hangzhou 310018, China; taoyuan0510@126.com

<sup>4</sup> Shining 3D Technology Co., Ltd., 1938 Xiangbin Road, Wenyan Street, Xiaoshan District, Hangzhou 311258, China; chenchenfu@shining3d.com (Z.C.); xiejinliang@shining3d.com (J.X.)

\* Correspondence: caoxiaoxiao@cuz.edu.cn

**Abstract:** Innovation products from historical cultural architectural have widely adopted 3D printing technology in recent years. To study the applicability of existing 3D printing materials, it is necessary to analyze the performance indicators of 3D printing materials and carry out material science experiments. Step 1: the material performance index composition of cultural innovation products was derived by integrating the literature of cultural heritage, product design, quality system, and material science. Step 2: The columns of Chengs' Miyake in Huizhou were taken as the creative source. Its geometric shape model was obtained through 3D scanning, and the design of the cultural innovation products was completed. Step 3: Photosensitive resin, nylon, and stainless steel, three commonly used 3D printing materials, were used to make samples, with one sample of each material. Finally, we carried out material science tests according to the material performance index. The experimental data of three materials were obtained and compared. The properties of the three 3D printing materials, photosensitive resin, nylon, and stainless steel, have advantages and disadvantages. Still, they all struggle to meet the needs of cultural and creative products in historical buildings. It is necessary to integrate the three materials' properties to develop new 3D printing materials.

**Keywords:** historical architecture; cultural innovation products; 3D printing; material research



**Citation:** Hu, H.; Cao, X.; Zhang, T.; Chen, Z.; Xie, J. Three-Dimensional Printing Materials for Cultural Innovation Products of Historical Buildings. *Buildings* **2022**, *12*, 624. <https://doi.org/10.3390/buildings12050624>

Academic Editor: Shazim Ali Memon

Received: 31 March 2022

Accepted: 6 May 2022

Published: 8 May 2022

**Publisher's Note:** MDPI stays neutral with regard to jurisdictional claims in published maps and institutional affiliations.



**Copyright:** © 2022 by the authors. Licensee MDPI, Basel, Switzerland. This article is an open access article distributed under the terms and conditions of the Creative Commons Attribution (CC BY) license (<https://creativecommons.org/licenses/by/4.0/>).

## 1. Introduction

In 1972, the 17th session of the UNESCO General Conference in Paris adopted the “Convention for the Protection of the World Cultural and Natural Heritage” [1], proposing that historical buildings belong to the cultural heritage of all humankind. The cultural values contained in historical buildings are usually maintained and managed in museums in most countries around the world [2]. Since the 1950s, museums in Europe and the United States have begun to raise funds by developing and selling museums derivatives. In 1955, the United States established the Museum Store Association [3]; American marketing scientists Philip Kotler and Neil Kotler edited and published “Museum Strategy and Marketing” [4]. Since 2010, world-renowned museums represented by the British Museum in the United Kingdom, the Metropolitan Museum in the United States, the National Palace Museum in Taipei, and the Palace Museum in Beijing have promoted the development of cultural innovation products of various historical buildings by authorizing images and brands of cultural relics and developing derivatives of cultural relics [5].

To preserve the cultural authenticity of historical buildings [6], the development of cultural innovation products for historical buildings primarily uses 3D scanning technology to obtain digital models of building components [7], then carries out the creative design based on the digital models, and finally uses 3D printing for production. For example, in

2014, the British Museum cooperated with Sketchfab to launch a 3D printing service for 14 collections, including the Caesar Marble statue [8].

Three-dimensional printing technology is increasingly used in the construction industry. Scholars Nils O.E. Olsson, Emrah Arica, Ruth Woods, and others from the Norwegian University of Science and Technology conducted research and analysis on the project management of 3D-printed concrete in building construction [9]. Scholars Max Adaloudis and Jaime Bonnin Roca from the Eindhoven University of Technology in the Netherlands analyzed the carbon footprint and sustainable development benefits of 3D concrete printing technology [10]. Scholars Richard Buswell, Jie Xu, and Daniel De Becker from the University of Sheffield in the United Kingdom researched the measurement benchmarks and tolerances of 3D-printed concrete parts for construction [11].

As an additive manufacturing process, 3D printing can achieve many forms that subtractive manufacturing processes cannot complete. Direct production can be reached as long as there is a digital model. It has almost no restrictions on materials; plastic, metal, wood, and ceramics can all be used. In the process of using 3D printing to develop historical buildings' cultural innovation products, the choice of materials is essential [12].

From various references [2–11], the current research on historical buildings' innovation products mainly focuses on museum marketing and product design. In contrast, the research on 3D printing materials primarily focuses on the physical and chemical properties of 3D printing materials, the preparation process, etc. However, there is insufficient research on the cultural properties and the combination of cultural and practical properties in cultural innovation products. This paper carried out the following study: (1) According to the existing literature on cultural heritage, product design, quality systems, and materials science research, we discussed and analyzed the material index composition of historical buildings' cultural innovation products. (2) We collected the original morphological data of historical building components through 3D scanning, developed digital models of cultural innovation products, and then used three different 3D printing materials to make experimental samples. (3) We carried out material science tests, obtained test data of three materials, compared the data, analyzed the performance of materials according to the requirements of material performance indicators, and received research conclusions.

## 2. Materials and Methods

### 2.1. Research on Material Indicators of Historical Buildings' Cultural Innovation Products

Because the development of historical buildings' cultural innovation products needs to consider the cultural value of historical buildings and the practical properties of physical products at the same time, the paper adopted the three levels of "design theory level–quality system level–performance indicator level" and the two dimensions of "cultural dimension–practicality dimension". Documents in many research fields, such as cultural heritage authenticity [13], Kansei engineering [14], TRIZ contradiction solution [15], and so on, deduce the material index composition of historical buildings' cultural innovation products, as shown in Figure 1 below.

#### 2.1.1. Design Theory Level

At the design theory level in Figure 1, the design theories related to historical buildings' cultural innovation products include cultural authenticity theory and product design theory. Cultural authenticity theory includes architectural heritage authenticity [16] and user experience authenticity [17] (Cultural Tourism), which belongs to the cultural dimension. The field of product design can be divided into two parts: perceptual design and practical design, among which product design theories such as design semiotics [18], Kansei engineering, and design psychology [19] take into account cultural aspects dimensions and practical dimensions, while theories such as function-behavior-structure mapping [20], QFD quality house [21], and TRIZ contradiction solution belong to the practical dimension, and theories closely related to 3D printing materials research are shown in the figure with a purple background callout.

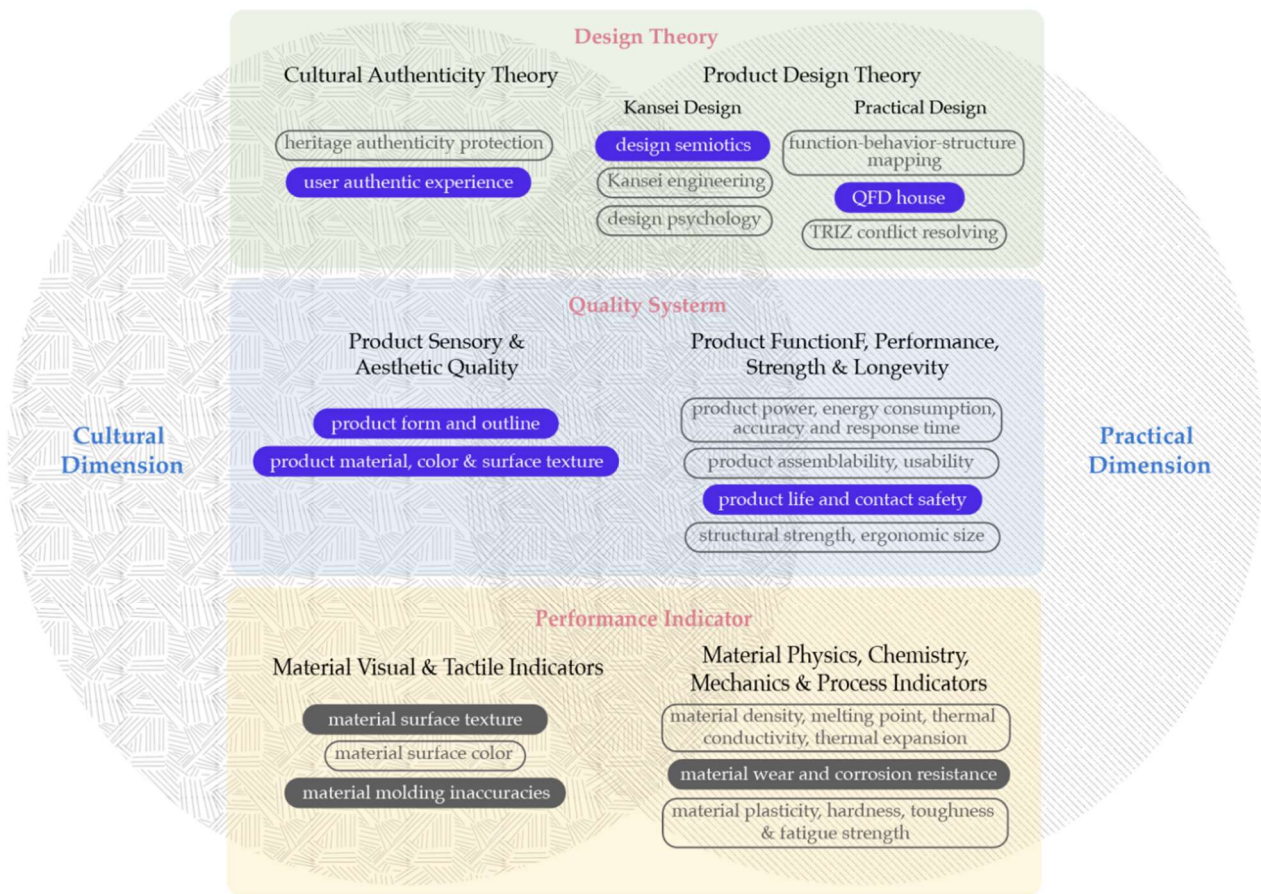


**Figure 1.** Material index derivation of historical buildings' cultural innovation products.

### 2.1.2. Quality System Level

In Figure 1, from the design theory to the quality system, the product quality of the cultural dimension refers to the sensory and aesthetic quality of the product, including product shape, outline, and quality indicators such as material, color, and surface texture. In contrast, the practical dimension of product quality refers to product function, performance, strength, and life, including product power, energy consumption, accuracy, response time, product assimilability, usability, product life, contact safety, structural strength, ergonomic dimensions, and so on, among which the relevant quality indicators closely related to 3D printing materials are marked with a purple background in the figure.

### 2.1.3. Performance Indicator Level

In Figure 1, deriving from the quality system to the performance indicator, the cultural dimension material index refers to the visual and tactile index of the material, including the surface texture and color of the material surface; the material index of the practical dimension refers to the material's physical properties, as well as chemical, mechanical and technological indicators. Among them, the material indicators related to 3D printing materials are distinguished by the dark grey background in the figure. The material process forming inaccuracy in Figure 1 refers to the geometric error of the finished product and the design model caused by different 3D printing materials (processes) for the same 3D digital model. The smaller the forming inaccuracy, the closer the material's surface texture is to the historical building relics, and the more the authenticity of the historic building can be preserved. Historical buildings' cultural innovation products, as practical products, will constantly contact with environmental media such as skin, moisture in the air, and acid and alkali during prolonged use, resulting in product wear and corrosion, affecting product life and contact safety.

#### 2.1.4. Material Performance Indicator

According to Figure 1, three material performance indicators for cultural innovation products of historical buildings were finally deduced and used as the basis for carrying out material science experiments. The first material performance indicator is the surface texture of the material. The closer the surface texture of the material is to the historical building relics, the better the visual authenticity of the historic building can be preserved. The second material performance indicator is the forming inaccuracy. The smaller the forming inaccuracy, the more authentic the shape of the historic building can be preserved. The third material performance indicator is the wear resistance and corrosion resistance of the material, which can ensure the product's service life. The above three material performance indicators were used as the basis for conducting 3D printing material experiments.

Forming inaccuracies are caused by different materials' physical and chemical properties and the corresponding 3D printing process. Material surface texture refers to the visual and tactile texture formed by a specific material after the 3D printing and post-processing processes. Material wear and corrosion occur when the product interacts with people and the environment during use. The three typical materials of nylon, photosensitive resin, and stainless steel were selected according to the inorganic (metal) and organic (plastic) dimensions; the three conditions of smooth, moderate, and rough; and the requirements of technology and process commonly used in the market for experiments later in the paper.

#### 2.2. Three-Dimensional Printing Material Experiment of Cultural Innovation Products in Historical Buildings

In order to verify the correctness and feasibility of the three material performance indicators proposed in Section 2.1.4, three common 3D printing materials, namely, photosensitive resin, nylon, and stainless steel, were selected. The material science experiments were carried out according to two steps: (1) test sample preparation and (2) 3D printing material test, to obtain experimental data and conduct research.

##### 2.2.1. Experimental Sample Preparation Historic Building Components—Plinth

In the wooden frame system of traditional Chinese buildings, wooden columns set off the weight of the upper beams and roofs of the building. To prevent water from eroding wooden columns, stone plinths are installed at the bottom [22] to connect the ground and the plinth. The structure is shown in Figure 2a. The figures in Figure 2 were drawn based on photographs taken in the field by the author. The plinth has two parts that are hidden underground and protrude from the ground. In general, the plinth refers to the part that protrudes from the ground. Because the plinth is located at the focus point of sight, it is often decorated with patterns such as an auspicious animal, lotus, flowers and grass, a dragon, and a phoenix. The stone plinths studied in this paper come from Cheng's Miyake [23] Museum during the Chenghua period of the Ming Dynasty (1465–1487 AD), as shown in Figure 2b, which is national fundamental cultural relics protection unit, now located in Huangshan City, Anhui Province, China. The plinth material was carved with contemporary indigenous tea garden stone [24] and Huizhou stone carving [25] techniques. The building structure on the upper part of the plinth includes wooden columns, shuttle-like columns, and railings (on the second floor).



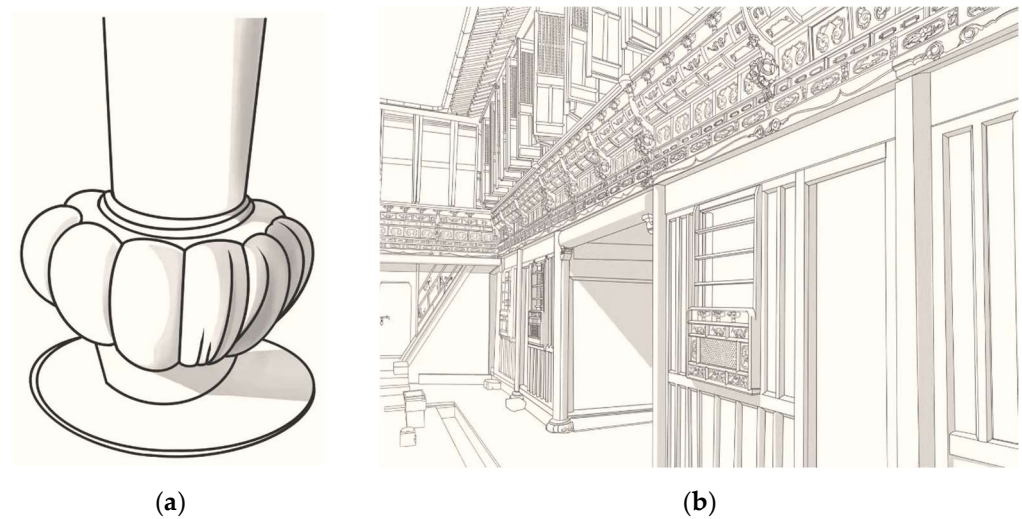


**Figure 2.** (a) Structure of stone plinth; (b) foyer and patio of Cheng's Miyake Museum.

#### Plinth Data Collection

Data collection method: Cultural innovation products of historic buildings need to retain the cultural authenticity of the original building components as much as possible, especially the decorative patterns in the form of curved surfaces. For this reason, in the Cheng's Miyake, complete stone carving plinths are selected for 3D scanning to obtain stone carvings. The original geometric data of the plinths are shown in Figure 3 below (hand-painted by the authors).

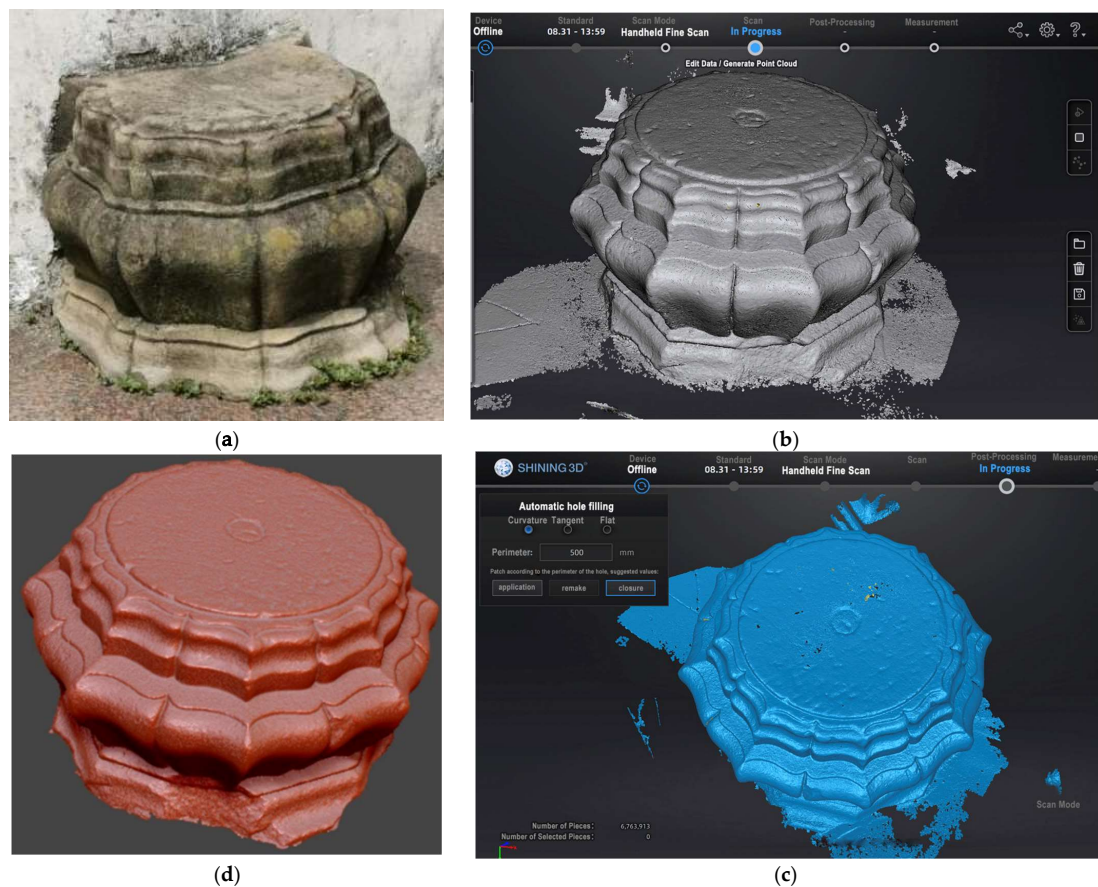


**Figure 3.** (a) Stone plinth cultural relics; (b) scanned point cloud data of stone plinth; (c) patching point cloud data; (d) plinth digital model.

Technical parameters of data collection: The equipment used for 3D scanning is a multifunctional handheld 3D scanner from China Shining 3D Technology Co., Ltd. (Hangzhou, China). The equipment model is EinScan Pro 2X Plus, the light source is white LED, and the scanning speed is 20 fps, 1,100,000 points/second. The scanning accuracy is 0.05 mm, the spatial point distance is 0.2 mm~3 mm, and the single-sided scanning range is 208 mm × 136 mm ~312 mm × 204 mm.

The experimental process of data acquisition is as follows:

1. Use a handheld 3D scanning device to collect data at Cheng's Miyake field and synchronously transfer it to the workstation of the laptop, as shown in Figure 3a;
2. Select the fine scan mode and start scanning. Figure 3b shows the scanned point cloud data.
3. Convert the point cloud data into three-dimensional data in the form of three points, where each three points form one surface, and then use software to repair the deep holes or corners that have not been scanned, as shown in Figure 3c;
4. Use the software EXSCAN pro [26] to complete the data repair of the lotus petal column foundation, as shown in Figure 3d.

It can be seen that the digital model of the column foundation after the repair is very delicate, and the weathering damage and carving marks on the plane are genuinely preserved. The digital model of the column foundation is compatible with OBJ, STL, ASC, PLY, P3, 3MF, and other formats and can be directly exported to Rhino, 3DMAX, Zbrush, and other 3D modeling software.

### 3D Printing Production of Plinth Cultural Innovation Products

Experimental sample design: To preserve the cultural authenticity of the stone carving plinth, the geometric shape of the lotus-patterned surface of the plinth needs to be preserved in the design. Therefore, the digital model of the plinth is cut by one-fourth, and the face pieces are converted into entities. Figure 4a below shows a desktop paperweight product formed with four planes + one lotus petal curved surface. The dimensions of the product length × width × height are 89.19 × 84.24 × 86.24 (mm), respectively.

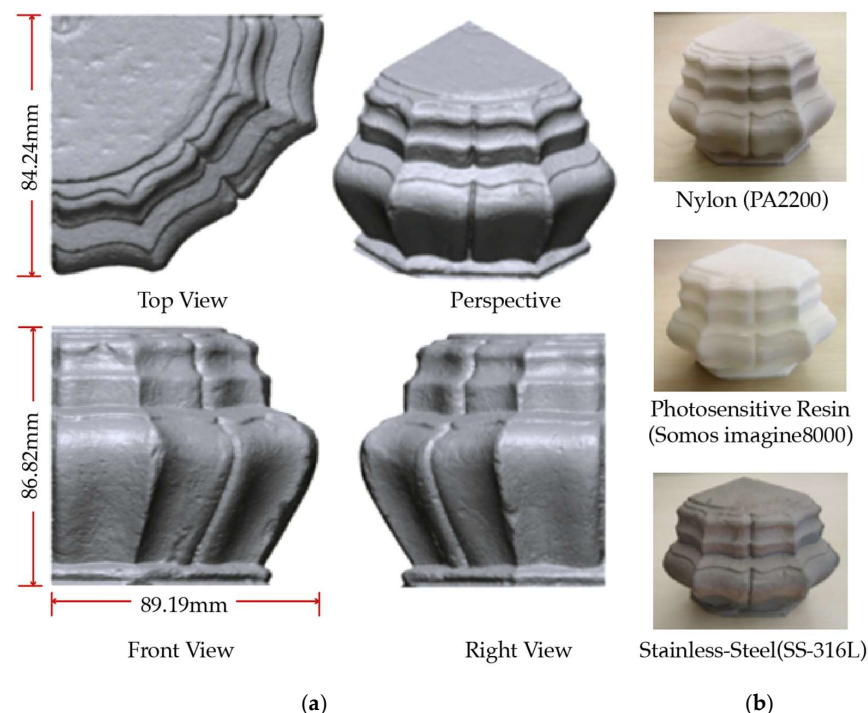


**Figure 4.** (a) Design model of stone plinth cultural innovation products; (b) 3D printing experimental samples.

According to the criteria discussed in Section 2.1.4, three commonly used 3D printing materials were selected. For each material, one sample was made with corresponding processes. The production process is as follows: (1) Nylon [27] (model PA2200)—produced by a laser sintering process, with the following process parameters: average grain size of 56  $\mu\text{m}$  (ISO 13320-11), layer thickness of 0.12 mm, and scanning speed 15 m/s. (2) Photo-sensitive resin [28] (model Somos imagine8000)—produced by a photocuring process, with the following process parameters: scanning speed of 8 m/s, spot size of 0.10 mm, and layer thickness of 0.15 mm. (3) Stainless steel [29] (model SS-316 L)—produced by a powder melting process, with the following process parameters: layer thickness of 30  $\mu\text{m}$ , spot diameter of 70  $\mu\text{m}$ , scanning speed of 5 m/s, and molding speed of 15  $\text{cm}^3/\text{h}$ , as shown in Figure 4b.

## 2.2.2. Comparative Experiment of 3D Printing Materials

After obtaining the three samples shown in Figure 4b, we reconsidered Figure 1 and the three material performance indicators proposed in Section 2.1.4—(1) material surface texture, (2) Forming inaccuracy, and (3) wear resistance and corrosion resistance. The following three material experiments were carried out in sequence.

As the creative prototype, the stone carving plinth is a national cultural relic that cannot be transported, and surface texture testing cannot be carried out directly. After the preparation of the experimental samples, the comparison of the surface texture indicators in Figure 1 can only be made through vision and touch. Visual and tactile experiments of surface texture were carried out on the samples of the three materials shown in Figure 4b.

### Forming Inaccuracy Experiment of 3D Printing Materials

Experiment principle: To compare the forming inaccuracy of the three materials in Figure 4b, three-dimensional scanning technology was used again to scan the experimental samples, and the geometric data were obtained in the three-dimensional inspection software. Compared with the design data of Figure 4a [30], the forming inaccuracy of different materials (processes) was checked.

Experimental process:

1. Three-dimensional scanning to collect data: put three experimental samples of different materials on a rotatable worktable and use an industrial-grade high-precision 3D inspection scanner (model OKIO 5M) for data sampling and to obtain the 3D geometric data of the three experimental samples, as shown on the left side of Figure 5a.
2. Three-dimensional data inspection and comparison: Import the 3D geometric model of the experimental sample obtained by 3D scanning into Geomagic® Control X 3D inspection software and analyze the difference between the imported geometric model and the geometric model of the initial design, as shown in Figure 5. The colored model in Figure 5b represents the geometry of the experimental sample obtained after 3D scanning. By comparing the size of the uniformly distributed sampling points on the surfaces of the two models, the geometric dimensions of this model and the design model in Figure 4a are compared. Since the 3D printing process will produce forming inaccuracies, the dimensional errors on the experimental samples are visualized in different colors. The green area indicates that these sampling points' inaccuracies range (within 0.1 mm) is reasonable. Yellow and red indicate a positive error in these sampling points, where Figure 5b is larger than the design model size of Figure 4a; on the other hand, light blue and dark blue represent negative errors at these sampling points, where Figure 5b is smaller than the design model size of Figure 4a.

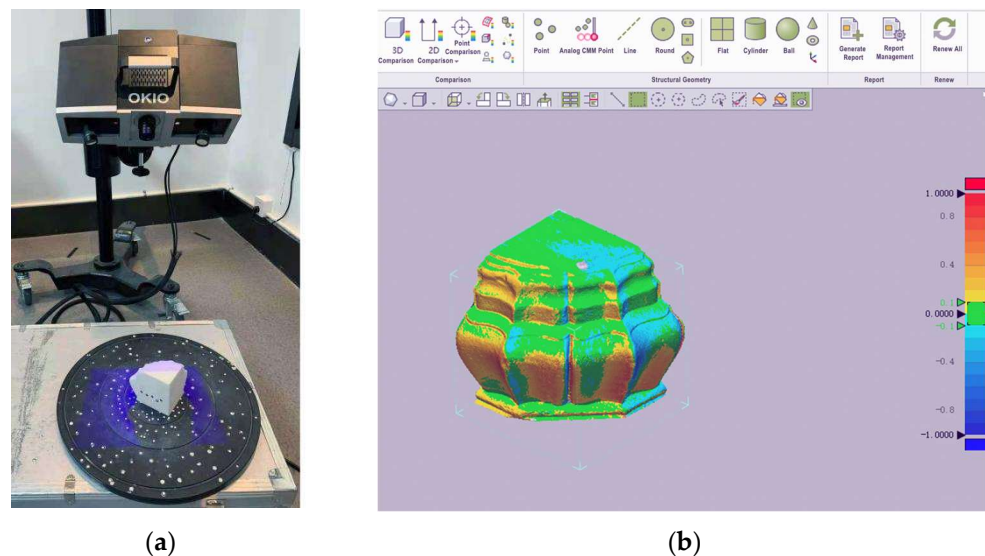


**Figure 5.** (a) Three-dimensional scanning of experimental samples; (b) experiment sample forming inaccuracy detection.

### Wear and Corrosion Resistance Test of 3D Printing Materials

**Experiment principle:** In the laboratory environment, zirconia ceramic balls, acid, alkali, and salt solutions were used to simulate samples' wear and corrosion resistance of three different materials—photosensitive resin, nylon, and stainless steel.

**Experimental process:**

1. The wear resistance experiment was carried out regarding the method in the literature [31,32]: zirconia ceramic balls were used to roll friction on the surface of the experimental sample. The duration was 30 min, the frequency was 2 Hz, the load was 5 N, the ambient temperature was 25 °C, and the ambient humidity was 60%;
2. The corrosion resistance test mainly investigates the stability of the samples in acid, alkali, and salt environments. It was carried out concerning the method in the literature [33,34]: the samples were respectively immersed in HCl dilute solution (0.25%) and NaOH dilute solution (0.1 g/mL), and soaked in NaCl dilute solution (0.1 g/mL) for 72 h. Before and after the experiments, the surfaces of the samples were cleaned and observed with a microscope.

## 3. Result

### 3.1. Results of Surface Texture Experiment

As shown in Figure 1, the material's surface texture is a material performance index belonging to the cultural dimension. Comparing the surface textures of the three 3D printing materials through vision and touch, it can be concluded that the surface textures of nylon and stainless steel are relatively rough, which is closer to the original texture of the stone plinth in Figure 3. On the other hand, the photosensitive resin is delicate and smooth, which is closer to the texture of contemporary organic materials (plastics). The SEM morphology [35] of the three materials shown in Section 3.3. can also illustrate this point. The texture of stainless steel is closest to the mottled surface texture of historical building components (stone, wood, etc.) that have been weathered for a long time. Therefore, from the cultural perspective of preserving the authenticity of historical buildings, stainless steel is better than nylon, and nylon is better than photosensitive resin.

### 3.2. Validation of Inaccuracy Levels

According to Figure 5, the frequency distribution diagrams of forming inaccuracies of three different 3D printing materials can be obtained, as shown in Figure 6 (supplied by the three-dimensional inspection software Geomagic® Control X). The abscissas in Figure 6a–c



represents the error distribution between the test sample and the design model, that is, the size difference of the sampled data points between Figures 4a and 5b. The middle of the abscissa is the average error value. The positive and negative values symmetrical to the left and right sides are not the maximum and minimum errors but are used to better express the value of the frequency distribution interval. The maximum and minimum errors are shown in Table 1a–c. The unit of abscissa is mm. The ordinate in the figure represents the frequency corresponding to the size error, but the specific frequency value is not given in the figure. Still, the frequency distribution’s statistical percentage (%) is shown. That is, the sum of the frequencies of a specific size error interval accounts for the percentage of the total sum of frequencies. This drawing method is more intuitive than giving specific frequency values. Corresponding to Figure 6a–c, the specific statistics of the forming inaccuracies of the three experimental samples are provided in Table 1a–c. The minimum, maximum, average value, root mean square (RMS), and standard deviation in the table are all generated for the size errors of sampled data points that are uniformly distributed on the surfaces of the two models in Figures 4a and 5b. The unit is mm.

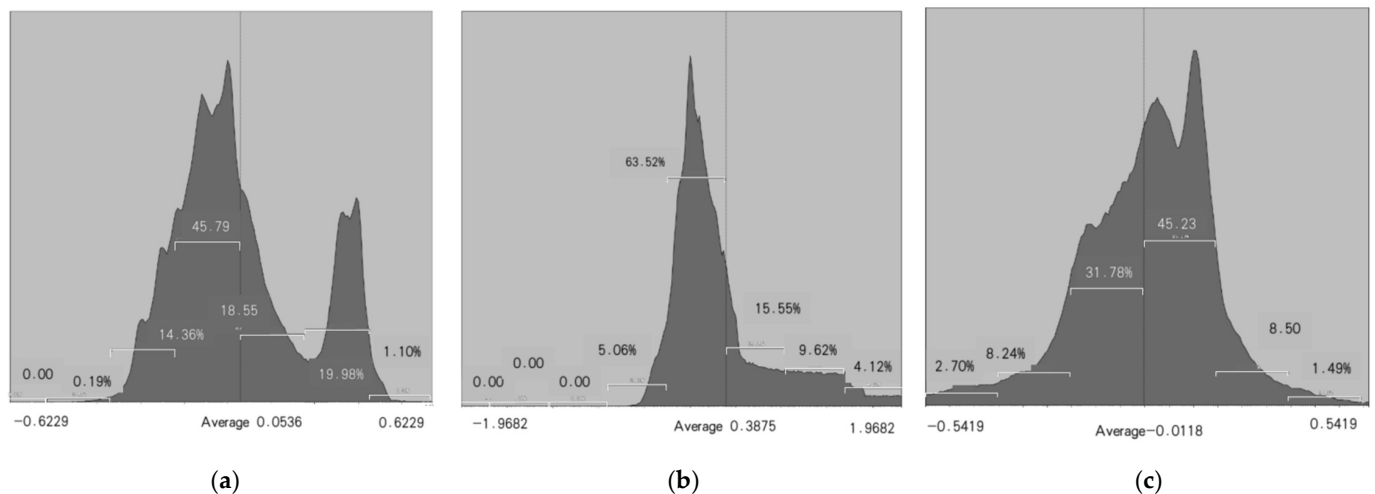


**Figure 6.** (a) Stainless steel forming inaccuracies frequency distribution diagram (frequency percentage); (b) photosensitive resin forming inaccuracies frequency distribution diagram (frequency percentage); (c) nylon forming inaccuracies frequency distribution diagram (frequency percentage).

**Table 1.** (a) Stainless steel forming inaccuracies statistics; (b) photosensitive resin molding inaccuracies statistics; (c) nylon molding inaccuracies statistics.

Stainless-Steel (a)		Photosensitive Resin (b)		Nylon (c)	
Minimum(mm)	−0.8093	Minimum (mm)	−1.113	Minimum (mm)	−0.7576
Maximum(mm)	0.818	Maximum (mm)	2.3501	Maximum (mm)	0.7548
Average (mm)	0.0536	Average (mm)	0.3875	Average (mm)	−0.0118
Standard Deviation (mm)	0.1897	Standard Deviation (mm)	0.5269	Standard Deviation (mm)	0.1767
Discrete (mm)	0.036	Discrete (mm)	0.2776	Discrete (mm)	0.0312
Within Tolerance (%)	47.2202	Within Tolerance (%)	26.5679	Within Tolerance (%)	47.2897
Out of Tolerance (%)	52.7798	Out of Tolerance (%)	73.4321	Out of Tolerance (%)	52.7103
Above Tolerance (%)	31.7399	Above Tolerance (%)	66.3077	Above Tolerance (%)	26.4588
Below Tolerance (%)	21.0399	Below Tolerance (%)	7.1245	Below Tolerance (%)	26.2515

In-tolerance, out-of-tolerance, above-tolerance, and below-tolerance values refer to the percentage of the frequency distribution of dimensional errors, and the unit is percentages. Figure 6 and Table 1 show that the forming errors of the two test samples made of nylon and stainless steel are not much different, but the various inaccuracies of photosensitive resin are more significant than those of nylon and stainless steel. From the two indicators of above-tolerance (%) and below-tolerance (%) values, photosensitive resin’s deformation

generates a positive error, stainless steel also mostly generates a positive error, and the positive and negative inaccuracies of nylon material are basically equal. As shown in Figure 1, the material's surface texture is a material performance index belonging to the cultural dimension. Comparing the surface texture of the three 3D printing materials by visual and tactile sense, it can be concluded that the surface texture of nylon and stainless steel is relatively rough, which is closer to the original texture of the stone carving pillar in Figure 3. On the other hand, the photosensitive resin is delicate and smooth, which is closer to the texture of contemporary organic materials (plastics). The SEM morphology of the three materials shown in Figure 7a1,b1,c1 can also illustrate this point. The texture of stainless steel is closest to the mottled surface texture of historical building components (stone, wood, etc.) that have been weathered for a long time. Therefore, from the cultural perspective of preserving the authenticity of historical buildings, stainless steel is better than nylon, and nylon is better than photosensitive resin.

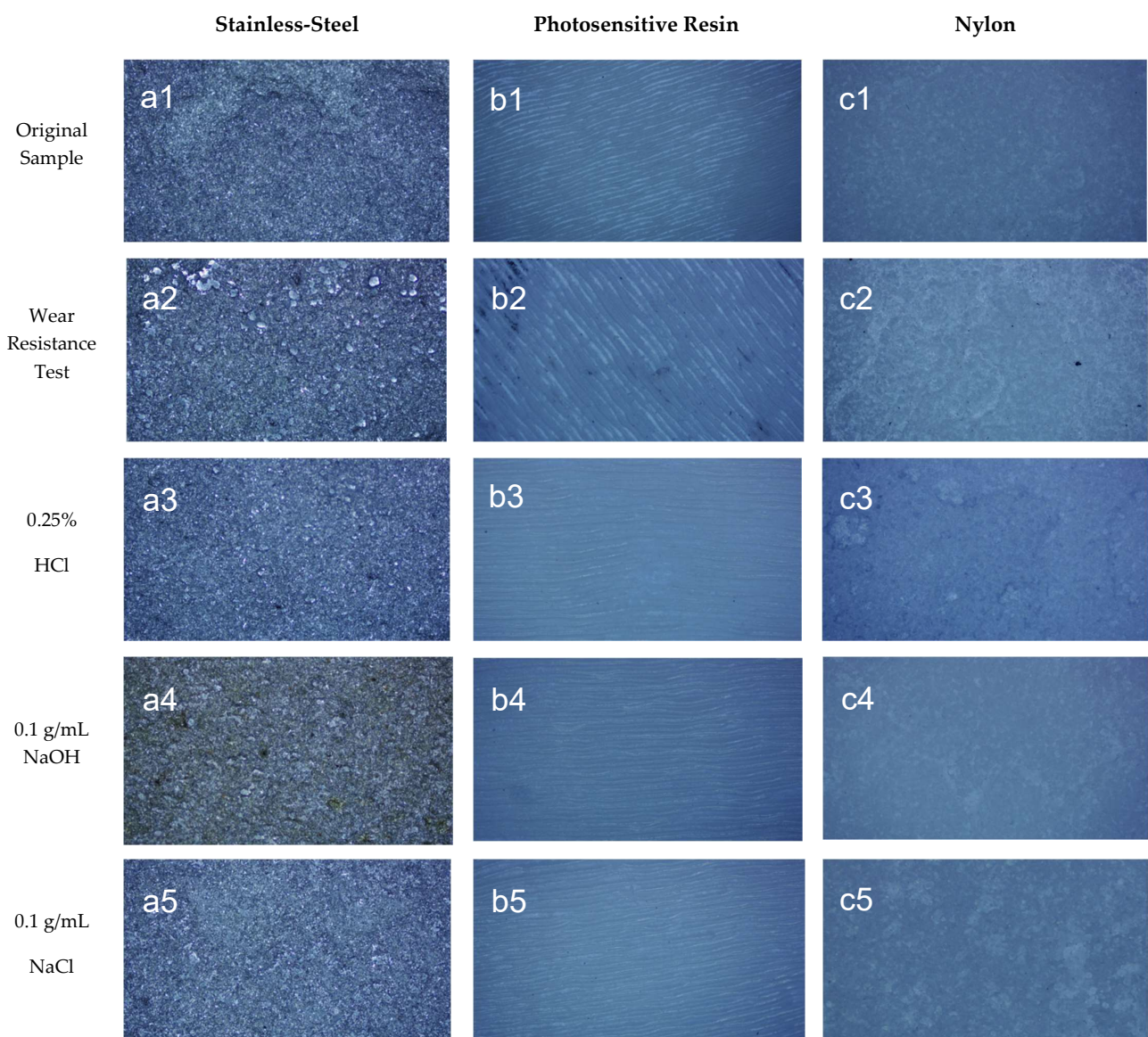


**Figure 7.** (a1–c1) Surface morphologies of stainless steel, photosensitive resin, and nylon; (a2–c2) Material surface morphologies after wear resistance tests; (a3–c3) Material surface morphologies after 0.25% HCl dilute solution corrosion test; (a4–c4) Material surface morphologies after 0.1 g/mL NaOH dilute solution corrosion test; (a5–c5) Material surface morphologies after 0.1 g/mL NaCl dilute solution corrosion test.

### 3.3. Experiment Results of Wear and Corrosion Resistance of 3D Printing Materials

After the rolling friction of the zirconia ceramic ball, the pattern on the surface of the photosensitive resin sample appeared discontinuous, indicating that the surface was worn, as shown in Figure 7b2. In contrast, the degree of surface wear of the nylon sample is not apparent, as shown in Figure 7c2.

After being immersed in 0.25% HCl dilute solution for 72 h, the surface texture of the photosensitive resin sample becomes lighter or even disappears intermittently, as shown in Figure 7b3; the surface of the nylon sample also appears to be damaged to a certain extent. Multiple blocky plaques appeared on the surface, as shown in Figure 7c3; in contrast, there was no apparent corrosive damage on the surface of the stainless steel sample, as shown in Figure 7a3.

After soaking in 0.1 g/mL NaOH dilute solution for 72 h, the surface of the photosensitive resin and nylon samples showed no apparent damage, showing better stability, as shown in Figure 7b4,c4. The surface of the stainless steel sample showed noticeable color change, which may be caused by the corrosive damage of the alkaline solution, as shown in Figure 7a4. After being soaked in 0.1 g/mL of the NaCl diluted solution for 72 h, the surface texture of the samples made of stainless steel, photosensitive resin, and nylon did not change significantly, showing good stability, as shown in Figure 7a5,b5,c5.

As shown in Figure 1, wear resistance and corrosion resistance are the material performance indicators that belong to the dimension of product practicality. As practical products, cultural innovation products of historical buildings will be in constant contact with environmental media such as skin, moisture in the air, acid, and alkali during use, resulting in product wear and corrosion, affecting product service life and safety of skin contact. It can be seen from the experimental data that the wear resistance of nylon material is good, while the corrosion resistance of stainless-steel material is also good, but the two material performance indicators of photosensitive resin are not ideal.

## 4. Discussion and Conclusions

With the development of cultural heritage protection and digital technology, 3D printing technology is widely used in products such as historical building cultural innovation products, museum cultural innovation products, and tourist souvenirs. Therefore, the performance of 3D printing materials has become one of the critical factors affecting the quality of cultural innovation products. The current research on historical buildings cultural innovation products by researchers mainly includes research from the perspectives of (1) museum operation and management, (2) development of cultural innovation industries, and (3) design of souvenirs authorized by historical buildings. Historical buildings' cultural innovation products are a relatively new research angle.

The current research on 3D printing materials in the construction industry mainly includes (1) construction technology and quality of 3D-printed concrete; (2) economic, social, and environmental benefits of 3D-printed concrete; and (2) construction project management of 3D-printed concrete to analyze 3D printing in construction from these perspectives. However, there is insufficient research on the cultural properties of 3D printing materials and the wear resistance and acid and alkali corrosion resistance during use. This paper combines the two fields of historical building culture, practical product needs, and materials to put forward a new research perspective.

Under the dual needs of cultural authenticity and product practicability, starting from the literature on cultural heritage, product design, quality systems, and materials science, the authors summarize and deduce three material performance indicators, surface texture, forming error, and wear resistance and corrosion resistance. These three material performance indicators are not complete and can be expanded and revised with the development of subsequent 3D printing processes and materials.

Nylon, photosensitive resin, and stainless steel are currently widely used materials. The comprehensive material experiment results show that stainless steel is better than nylon and photosensitive resins, but stainless steel has a high density and insufficient wear



resistance and is mainly used for mechanical parts rather than consumer goods. Therefore, none of the above three materials can perfectly meet the material requirements of cultural innovation products. It is necessary to integrate the properties of these three materials to develop new 3D printing materials for cultural and creative products.

The experimental research on the surface texture, forming inaccuracy, and wear resistance and corrosion resistance of 3D printing materials integrates the research paradigms of the three disciplines of design art, mechanical manufacturing, and materials science and has the characteristics of interdisciplinary research. The depth of research ideas and experimental methods is slightly insufficient. However, the research has corresponding reference value for related disciplines such as art design, 3D printing, and materials science. It enriches and develops research fields such as museology, product design, and 3D printing.

**Author Contributions:** Conceptualization, H.H. and X.C.; methodology, T.Z.; software, Z.C.; validation, X.C. and J.X.; formal analysis, X.C.; investigation, X.C.; resources, H.H.; data curation, T.Z.; writing—original draft preparation, H.H.; writing—review and editing, X.C.; visualization, X.C.; supervision, H.H.; project administration, H.H.; funding acquisition, H.H. All authors have read and agreed to the published version of the manuscript.

**Funding:** This research was funded by “National Cultural and Tourism Science and Technology Innovation Engineering Projects, grant number 2019-006” and “Humanities and Social Sciences Research Projects of Ministry of Education, grant number 18YJA760022”.

**Institutional Review Board Statement:** Not applicable.

**Informed Consent Statement:** Not applicable.

**Data Availability Statement:** Not applicable.

**Conflicts of Interest:** The authors declare no conflict of interest.

## References

- Helge, O.B.; Georg, P.; Øystein, B.T. Convention Concerning the Protection of the World Cultural and Natural Heritage (World Heritage Convention). In *Yearbook of International Cooperation on Environment and Development 1998–1999*; Routledge: London, UK, 1998; Volume 101, p. 2.
- Ahmad, Y. The Scope and Definitions of Heritage: From Tangible to Intangible. *Int. J. Herit. Stud.* **2006**, *12*, 292–300. [\[CrossRef\]](#)
- Chen, L. Research on The Development of Museum Cultural Creative Products. In *Doctor of Philosophy*; Shanghai University: Shanghai, China, 2019.
- Neil, G.K.; Philip, K.; Wendy, I.K. *Museum Marketing and Strategy: Designing Mission Building Audience Generating Revenue and Resources*, 2nd ed.; John Wiley & Sons: San Francisco, CA, USA, 2008.
- Jasim, M.A.; Hanks, L.; Borsi, K. Can Politically Oriented Interventions in Built Heritage Contribute to Its Authenticity? Erbil Citadel’s Babylonian Gate as a Case Study. *Built Herit.* **2021**, *5*, 10. [\[CrossRef\]](#)
- Yeong, W.S.; Jin, L.Y. A Study on 3D Printing Products/Service Users Focused on Shape Ways, an Online 3D Printing Service. *Des. Converg. Study* **2018**, *17*, 219–233.
- Li, L.; Tang, L.; Zhu, H.; Zhang, H.; Yang, F.; Qin, W. Semantic 3D Modeling Based on CityGML for Ancient Chinese-Style Architectural Roofs of Digital Heritage. *ISPRS Int. J. Geo-Inf.* **2017**, *6*, 132. [\[CrossRef\]](#)
- Desiderio, J.G.-A. Knowledge Transfer Processes in the Authenticity of the Intangible Cultural Heritage in Tourism Destination Competitiveness. *J. Herit. Tour.* **2019**, *14*, 409–421.
- Olsson, N.O.; Arica, E.; Woods, R.; Madrid, J.A. Industry 4.0 in a Project Context: Introducing 3D Printing in Construction Projects. *Proj. Leadersh. Soc.* **2021**, *2*, 100033. [\[CrossRef\]](#)
- Adaloudis, M.; Roca, J.B. Sustainability Tradeoffs in the Adoption of 3D Concrete Printing in the Construction Industry. *J. Clean. Prod.* **2021**, *307*, 127201. [\[CrossRef\]](#)
- Buswell, R.; Xu, J.; De Becker, D.; Dobrzanski, J.; Provis, J.; Kolawole, J.T.; Kinnell, P. Geometric Quality Assurance for 3D Concrete Printing and Hybrid Construction Manufacturing Using a Standardised Test Part for Benchmarking Capability. *Cem. Concr. Res.* **2022**, *156*, 106773. [\[CrossRef\]](#)
- Ciampi, G.; Spanodimitriou, Y.; Scorpio, M.; Rosato, A.; Sibilio, S. Energy Performances Assessment of Extruded and 3D Printed Polymers Integrated into Building Envelopes for a South Italian Case Study. *Buildings* **2021**, *11*, 141. [\[CrossRef\]](#)
- Lin, G.; Giordano, A.; Sang, K.; Stendardo, L.; Yang, X. Application of Territorial Laser Scanning in 3D Modeling of Traditional Village: A Case Study of Fenghuang Village in China. *ISPRS Int. J. Geo-Inf.* **2021**, *10*, 770. [\[CrossRef\]](#)
- Li, Z.; Song, L.; Xiao, J.; Ni, J. Research on modeling image of anchor chair Based on Kansei Engineering. *Packag. Eng.* **2021**, *42*, 239–246. [\[CrossRef\]](#)



15. Chybowska, D.; Chybowski, L. A Review of TRIZ Tools for Forecasting the Evolution of Technical Systems. *Manag. Syst. Prod. Eng.* **2019**, *27*, 174–182. [\[CrossRef\]](#)
16. Karlsson, H.; Gustafsson, A. Staging Antiquity: A Comparison of Five Greek Cultural Heritage Sites and The Construction of Their Authenticity. *J. Herit. Manag.* **2020**, *5*, 7–23. [\[CrossRef\]](#)
17. Kim, S.-H.; Kim, C.-W. An Exploration of Authenticity and the Visit Experience at the Arts Tourism Destination: A Narrative Analysis of Travel Blogs. *J. Tour. Sci.* **2019**, *43*, 137–158. [\[CrossRef\]](#)
18. Domingues, F.; Zingale, S.; De Moraes, D. Aesthetics in Design Semiotics Research. Developing Foundations to Better Comprehend Cultural Habits and Codes in Bottom-up Design Processes. *Design J.* **2017**, *20* (Suppl. 1), S49–S62. [\[CrossRef\]](#)
19. Chi, Y.; Zhang, J. Summarize the Application and Development of Psychology in the Subject of Design. *Inter. J. Front. Eng. Tech.* **2021**, *3*, 30–34. [\[CrossRef\]](#)
20. Zhou, Q.; Li, X.; Zhou, J. Innovative Design Method for Integration of Fuzzy Kano and Situational FBS Model. *J. Graph.* **2020**, *41*, 796–804.
21. Putri, A.; Setyawan, P.; Diyas, Y.; Ari, A. Integrated Hand Cleaner and Dryer Product Design Using QFD as a Solution for New Normal Era. *Int. J. Invent. Eng. Sci.* **2020**, *6*, 1–3.
22. Pan, Y.; An, R.; Wang, X.; Guo, R. Research on mechanical model of tenon joints in ancient wooden structure. *China Civ. Eng. J.* **2020**, *53*, 61–70. [\[CrossRef\]](#)
23. Bi, Z. A brief analysis of the architectural form of Cheng's three houses in Huizhou ancient folk houses. *J. Henan Inst. Sci. Technol.* **2014**, *42*, 29–33.
24. Wu, A. *Tea Garden Stone*. 2018. Available online: [https://www.sohu.com/a/245936647\\_802636](https://www.sohu.com/a/245936647_802636) (accessed on 10 November 2021).
25. Chang, B. *Jiangnan Architectural Carving Art—Huizhou Volume*, 1st ed.; Southeast University Press: Nanjing, China, 2005.
26. EXSCAN Pro; Shining 3D Technology Co., Ltd.: Hangzhou, China, 2021.
27. Arnold, N.; Angelov, P.; Viney, T.; Atkinson, P. Automatic Extraction and Labelling of Memorial Objects From 3D Point Clouds. *J. Comput. Appl. Archaeol.* **2021**, *4*, 79–93. [\[CrossRef\]](#)
28. Fuentes, J.M.; Unda, O.F.; Ferrandiz, S.; Suarez, F. Effects of Steam Heat and Dry Heat Sterilization on Thermal and Mechanical Properties of Nylon and Polycarbonate in Fabrication with Fused Filament. *Key Eng. Mater.* **2021**, *891*, 150–163. [\[CrossRef\]](#)
29. Tessanan, W.; Daniel, P.; Phinyocheep, P. Development of Photosensitive Natural Rubber as a Mechanical Modifier for Ultraviolet-Curable Resin Applied in Digital Light Processing-Based Three-Dimensional Printing Technology. *ACS Omega* **2021**, *6*, 14838–14847. [\[CrossRef\]](#) [\[PubMed\]](#)
30. Shatagin, D.; Anosov, M.S.; Kolchin, P.; Ryabov, D.A.; Kiselev, A.V. Cold Resistance and Mechanical Properties of 07Cr25Ni13 (ER309LSI) Stainless Steel Obtained by 3D Printing by Electric Arc Surfacing on a CNC Machine. *Mater. Sci. Forum* **2021**, *1037*, 65–70. [\[CrossRef\]](#)
31. Guo, Y.; Sohel, F.; Bennamoun, M.; Lu, M.; Wan, J. Rotational Projection Statistics for 3D Local Surface Description and Object Recognition. *Int. J. Comput. Vis.* **2013**, *105*, 63–86. [\[CrossRef\]](#)
32. Ma, X.; Wang, W.; Qi, X.; Yang, J.; Lei, Y.; Wang, Y. Highly Thermally Conductive Epoxy Composites with Anti-Friction Performance Achieved by Carbon Nanofibers Assisted Graphene Nanoplatelets Assembly. *Eur. Polym. J.* **2021**, *151*, 110443. [\[CrossRef\]](#)
33. Wang, X.; Xing, Z.; Hou, J.; He, W.; Liu, K. Effect of Adding Ceramic Powder on the Microstructure, Wear and Corrosion Resistance of NiCrBSi/WC Coating. *J. Mater. Res. Technol.* **2021**, *15*, 4010–4020. [\[CrossRef\]](#)
34. Liao, L.; Gao, R.; Yang, Z.H.; Wu, S.T.; Wan, Q. A Study on the Wear and Corrosion Resistance of High-Entropy Alloy Treated with Laser Shock Peening and PVD Coating. *Surf. Coat. Technol.* **2022**, *437*, 128281. [\[CrossRef\]](#)
35. Lv, L.; Zhang, J.; Xu, J.; Yin, J. Effects of Surface Topography of SiO<sub>2</sub> Particles on the Heterogeneous Condensation Process Observed by Environmental Scanning Electron Microscopy. *Aerosol Sci. Technol.* **2021**, *55*, 920–929. [\[CrossRef\]](#)